Direct Two-Dimensional Measurements of the Field-Aligned Current Associated with Plasma Blobs

I. Furno,[1] M. Spolaore,[2] C. Theiler,[1] N. Vianello,[2] R. Cavazzana,[2] and A. Fasoli[1]

[1]*Centre de Recherches en Physique des Plasmas, Ecole Polytechnique Fédérale de Lausanne (EPFL), Association EURATOM-Confédération Suisse, CH-1015 Lausanne, Switzerland*

[2]*Consorzio RFX, Associazione Euratom-ENEA sulla Fusione, Corso Stati Uniti 4, 35127 Padova, Italy*

(Received 17 January 2011; published 13 June 2011)

In simple magnetized toroidal plasmas, field-aligned blobs originate from ideal interchange waves and propagate radially outward under the effect of ∇B and curvature induced $\mathbf{E} \times \mathbf{B}$ drifts. We report on the first experimental two-dimensional measurements of the field-aligned current associated with blobs, whose ends terminate on a conducting limiter. A dipolar structure of the current density is measured, which originates from ∇B and curvature induced polarization of the blob and is consistent with sheath boundary conditions. The dipole is strongly asymmetric due to the nonlinear dependence of the current density at the sheath edge upon the floating potential. Furthermore, we directly demonstrate the existence of two regimes, in which parallel currents to the sheath do or do not significantly damp charge separation and thus blob radial velocity.

DOI: 10.1103/PhysRevLett.106.245001 PACS numbers: 52.35.Ra, 52.25.Fi, 52.35.Kt

Current structures associated with blobs and filaments are observed in natural and laboratory plasmas. Satellites reveal current filaments aligned with Earth's magnetic field [1], which are transported with ionospheric blobs. On RFX, a reversed field pinch, insertable magnetic probes measured field-aligned currents associated with blobs [2]. In tokamaks, current structures associated with filaments during edge localized modes (ELMs) were measured using fast imaging combined with external magnetic data on MAST [3], reciprocating magnetic probe data in the scrape-off layer (SOL) of ASDEX Upgrade [4] and JET [5], and filament modeling and comparison with external coil data on DIII-D [6]. Although the field-aligned nature of current filaments is a common feature, measurements of the two-dimensional (2D) structure in the plane perpendicular to the confining field are missing, thus preventing a fuller understanding of the origin of the current itself. Furthermore, to date, the importance of parallel currents on blob propagation is only indirectly inferred by comparing experimental blob speed-versus-size scalings [7,8] with theory predictions [9].

In this Letter, we report on the first 2D measurements of the parallel current density associated with radially propagating blobs in a simple magnetized toroidal plasma. The experiments are performed on the TORPEX device [10]. Blobs are generated from ideal interchange waves [11] and are propelled by the effective gravity force associated with ∇B and magnetic field curvature causing charge separation, polarizing the blob, and a corresponding radially outwards $\mathbf{E} \times \mathbf{B}$ drift [7,12]. Blobs propagate in a region where both of their ends are connected to a conducting limiter, where a plasma sheath is formed. Time-resolved 2D profiles of parallel current density to the limiter are obtained using data from a single-sided Langmuir probe (LP) and from a specially designed current probe, based on an array of magnetic pickup coils, which are conditionally sampled over many blob events. A dipolar structure of the parallel current density is revealed, which originates from blob-induced charge separation. This dipolar structure is consistent with sheath boundary conditions and is strongly asymmetric, resulting in a net current to the limiter. By using these internal measurements, we directly confirm the existence of two regimes [7], in which parallel currents to the sheath do or do not significantly damp charge separation, and thus blob radial velocity.

TORPEX (major radius $R = 1$ m, minor radius $a = 0.2$ m) plasmas are produced and sustained by microwaves ($P_{\mathrm{EC}} \approx 400$ W) in the electron cyclotron range of frequencies [13]. A vertical magnetic field $B_z = 1.6$ mT is imposed on a toroidal field of $B_t = 76$ mT, resulting in helical magnetic field lines with ∇B and curvature, that terminate on the lower and upper walls of the vessel. Consistently with theoretical predictions and numerical simulations [14], experimental measurements [15] reveal that plasma turbulence in the present configuration is dominated by an ideal interchange mode, localized around the position of maximum pressure gradient at $r \approx -3$ cm, with parallel, $k_{\parallel} \sim 0$, and perpendicular, $k_z = 2\pi/\Delta \approx 48\ \mathrm{m}^{-1}$, wave numbers. Here, $\Delta = 2\pi R B_z/B_t \approx 13$ cm is the vertical displacement of a field line after one toroidal turn. Similarly to the scenario in Refs. [7,11,16], blobs form from radially extending positive crests of the ideal interchange wave that are sheared off by the $\mathbf{E} \times \mathbf{B}$ flow. The radial elongation of the wave is attributed to an increased radial pressure gradient [11,17]. An example of the blob is shown in Fig. 1, generated using profiles of ion saturation current from a 2D LP array [18]. The elongation of the wave crest is shown in Fig. 1(b), while the radial

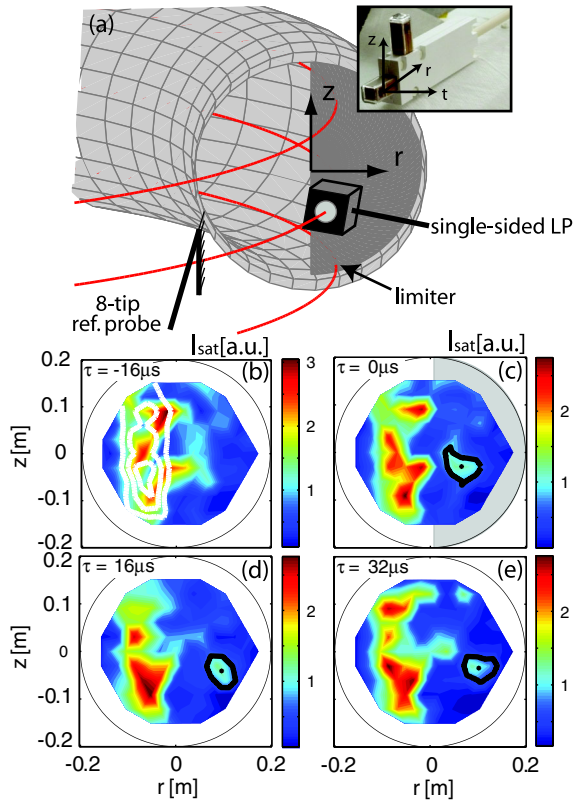

FIG. 1 (color online). (a) Schematics (not to scale) of the setup with a magnetic field line (in red [medium gray]) intercepting the limiter after one turn in the blob propagation region. Either the single-sided LP or the current probe (see the inset with the relevant coordinate system) is placed in front of the limiter. The eight-tip reference probe is toroidally displaced by ≈ 3 m from the limiter. (b)–(e) 2D profiles of ion saturation current from a 2D LP array, which is toroidally spaced by ≈ 90 degrees from the limiter. An example of a blob is highlighted by the thick black line.

propagation of the blob is clearly visible in Figs. 1(c)–1(e). For the present experiments, a steel limiter, schematically shown in Fig. 1(a), is inserted in the outer half of the cross section, i.e., $r > 0$, where blobs propagate. This defines a region where blobs are connected on both sides of the limiter with a nearly constant connection length $L_\parallel = 2\pi R \approx 6$ m [7], and perpendicular incidence, thus preventing contributions of the electron diamagnetic current to the blob parallel current [19].

In situ measurements of the parallel current density $J_\parallel$ constitute a challenging task in fusion plasmas. Various attempts have been performed and are now in progress [2,4,20]. Here, we use two different diagnostics: a single-sided LP, and a specially designed current probe. In the following, we define the fluctuating current density as $\tilde{J}_\parallel = J_\parallel - \bar{J}_\parallel$, where $\bar{J}_\parallel$ is the time-averaged current density. The first probe consists of a tungsten plate (8 mm in diameter, collecting area $A_{LP} \approx 50$ mm^2) with a single side exposed to the plasma. A schematic view of this probe is shown in Fig. 1(a). The plate is oriented perpendicularly to the magnetic field and is kept at the limiter potential, such that the current to the limiter, I_0, is measured by the probe. The current density is computed as $J_\parallel = I_0/A_{LP}$. The second probe consists of an L-shaped array of three miniaturized three-axial pickup coils (3.5 cm spaced, each with an effective area of 2.3×10^{-3} m^2). This arrangement is a simplified version of that used in the Cluster satellite to measure magnetospheric currents [21], and allows direct measurements of the fluctuating current density $\tilde{\mathbf{J}} = \mu_0^{-1} \nabla \times \tilde{\mathbf{B}}$. The current probe is oriented such that the (r, z) components of the magnetic field and their gradients along r and z are measured and the parallel current can be computed (inset in Fig. 1). The signals are digitized at 250 kHz.

Time-resolved 2D current density profiles are obtained by performing conditional sampling [22] over many blob events of the data in a time window centered around the blob detection. As schematically shown in Fig. 1, a multitip probe (8 tips, 1.8 cm spacing in the z direction), located at $r = 7$ cm and toroidally displaced by ≈ 3 m from the limiter, is used as a reference probe. This measures ion saturation signals, I_{ref}, which are used to detect blobs on the different tips, defined by the condition $\tilde{I}_{ref} \geq 3\sigma$, where σ is the standard deviation over the whole discharge. Two sets of measurements are performed, in which either the single-sided LP or the current probe is located in front of the limiter and toroidally displaced by 3 cm from it, as shown in Fig. 1. The probe is moved radially in between discharges, thus allowing reconstructing 2D profiles over a section of the r-z poloidal plane. Furthermore, 2D profiles of electron density n_e, temperature T_e, floating potential V_{fl}, and plasma potential $V_{pl} = V_{fl} + \Lambda T_e$ (the coefficient Λ is determined experimentally [13]) are measured in the same poloidal plane and in the bulk plasma at 1 m distance from the limiter, by using conditionally sampled I-V characteristics of a LP, which is moved between discharges [23].

Figure 2 illustrates the results of the conditional sampling of ≈ 3000 blobs over four identical, 1 s long plasma discharges in hydrogen. At the blob detection time and in a r-z plane located 3 cm in front of the limiter, we show the 2D profile of $J_\parallel$ from single-sided LP data, Fig. 2(a), and of $\tilde{J}_\parallel$ from current probe data, Fig. 2(b). The measurements from the two diagnostics are in excellent agreement, and single-sided LP measurements show that the time-averaged current density is small, such that $\tilde{J}_\parallel$-$J_\parallel \approx 1$ A m^{-2}. In the same plane, the 2D structure of the floating potential is shown in Fig. 2(c), together with the density blob (black contours) as detected in the bulk plasma, i.e., ≈ 1 m away from the limiter. The density blob is mapped onto the first plane by taking into account the vertical shift of the field line (≈ 2 cm) over the distance between the two planes. The electron density and temperature at the center of the blob are respectively $n_e \approx 1.4 \times 10^{16}$ m^{-3}

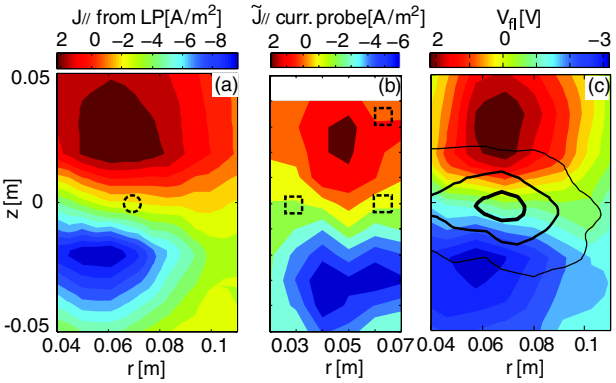

FIG. 2 (color online). At the time of the blob detection and measured ~3 cm in front of the limiter, 2D profiles of (a) $J_\parallel$ from the single-sided LP and (b) $\tilde{J}_\parallel$ from the current probe. For comparison with current structures, the dashed circle in (a) and dashed squares in (b) illustrate the single-sided LP collector and the arrangement of the current probe, respectively. Positive or negative currents correspond to an excess of ions or electrons collected by the limiter. (c) 2D floating potential in the same plane together with isocontours of blob density in the bulk plasma (1 m away from the limiter).

and $T_e \approx 2.5$ eV. The floating potential in Fig. 2(c) exhibits an almost perfectly symmetric dipolar structure, centered around the density blob, with $|V_{\rm fl}| \approx 3$ V at the positions of minimum and maximum values. Surprisingly, the current density dipolar structure is not symmetric, with a larger level ($J^- \approx -9$ A/m^{-2} at the minimum) of current flowing out of the limiter on the bottom of the blob than that ($J^+ \approx 2$ A/m^{-2} at the maximum) flowing into the limiter at the top of the blob. To understand this asymmetry, we display in Fig. 3 the 2D parallel current density at the sheath entrance as computed from (a) $J_\parallel = J_{\rm sat}\{1 - \exp[-e(V_{\rm pl} - \Lambda T_e)]/T_e]\} \equiv J_{\rm sat}[1 - \exp(-eV_{\rm fl}/T_e)]$ [24], where $J_{\rm sat} = 0.5 \times n_e e c_s$ is the ion saturation current density, and (b) from the linearized expression $J_\parallel \approx J_{\rm sat}[eV_{\rm fl}/T_e]$, under the assumption that $|eV_{\rm fl}/T_e| \ll 1$ [25]. Here, $c_s = \sqrt{T_e/m_i}$ is the ion sound speed and m_i the ion mass. While the exact expression in Fig. 3(a) is in excellent agreement with Figs. 2(a) and 2(b), displaying an asymmetric dipolar structure, the linearized version in Fig. 3(b) is almost perfectly symmetric. This is due to the assumption $|eV_{\rm fl}/T_e| \ll 1$, which is not satisfied here ($|eV_{\rm fl}/T_e| \approx 1$), such that the linearized expression leads to large errors in the $J_\parallel$ estimate. The asymmetry of the dipolar current density can be quantified by the ratio $\alpha = |J^-/J^+| = |[1 - \exp(-eV_{\rm fl}^{\rm min}/T_e)]/[1 - \exp(-eV_{\rm fl}^{\rm max}/T_e)]|$, where J^+ and J^- are the peak current densities in the positive and negative lobes, respectively. For $|eV_{\rm fl}/T_e| \approx 1$, we obtain $|J^-/J^+| \approx 2.7$, thus resulting in a net current to the limiter, which is carried by the electrons and exceeds the absolute value of the ion saturation current. Note that blobs commonly observed in fusion devices [26] have cross-field sizes $a \sim$ 1–3 cm and radial speeds $v_r \sim$ 0.5–2 km/s. An estimate of $V_{\rm fl} \sim a v_r B$ ($B \sim$ 1–5 T is the toroidal magnetic field of the device) indicates that $eV_{\rm fl} \sim$ 5–300 eV is in the range of SOL electron temperatures, thus suggesting that the current density asymmetry may be relevant also in these devices.

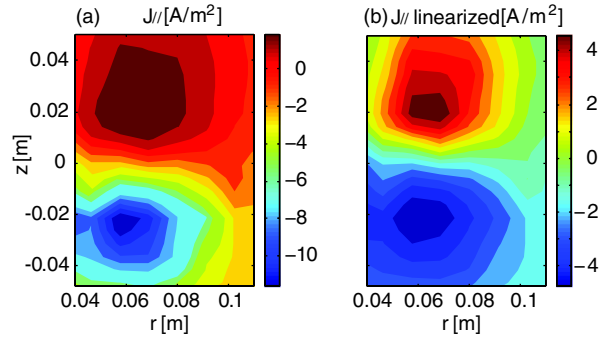

FIG. 3 (color online). Parallel current density (a) from sheath boundary condition $J_\parallel = J_{\rm sat}[1 - \exp(-eV_{\rm fl}/T_e)]$, and (b) from the linearized expression $J_\parallel \approx J_{\rm sat}[eV_{\rm fl}/T_e]$.

Next, we address the key question of the role of the parallel current in damping charge separation, and thus in determining the blob radial speed. In TORPEX, it was recently demonstrated that a statistical blob speed-versus-size scaling law, obtained by varying the ion mass, is consistent with the existence of two regimes, in which the blob speed is either limited by parallel current to the sheath or by ion polarization current [7]. Here, these two regimes, obtained for hydrogen and helium plasmas, are investigated with internal measurements.

Using a simple 2D model for the blob (i.e., $k_\parallel = 0$) [25,27], neglecting ion temperature ($T_i \ll T_e$ for TORPEX plasmas), and integrating $\nabla \cdot \mathbf{J} = 0$ along the magnetic field, we obtain the parallel current to the sheath required to completely damp the charge separation, in the absence of other closure paths for the current,

$$J_\parallel|_{\rm sheath} = -\frac{L_\parallel}{RB}\frac{\partial(n_e T_e)}{\partial z}\bigg|_{L/2}. \quad (1)$$

The right-hand side of Eq. (1) represents the drive for blob motion and is evaluated on a vertical cut across the density blob center from LP measurements in the bulk plasma (1 m away from the limiter) for hydrogen and helium blobs. The profiles are compared in Fig. 4 with the experimental profiles of the current density to the sheath. For hydrogen, Fig. 4(a), the profiles agree within the error bars for $z < 0$, demonstrating that parallel currents efficiently dissipate the charge separation in this region. This is not the case for $z > 0$ in hydrogen and for helium over the entire profile, Fig. 4(b), where other closure mechanisms, such as perpendicular ion polarization current and ion current due to neutral friction, must be effective to ensure $\nabla \cdot \mathbf{J} = 0$. We therefore conclude that parallel currents to the sheath damp

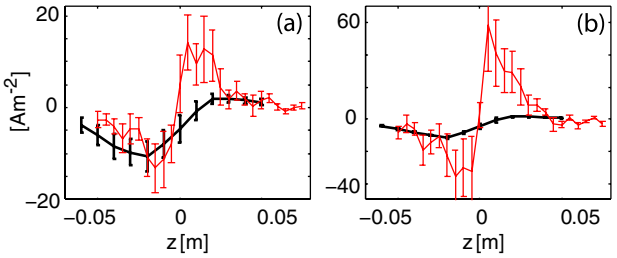

FIG. 4 (color online). Comparison of the measured parallel current density to the sheath (thick black line) with the profile from Eq. (1) (thin red line) reveals that the former is effective in damping charge separation in hydrogen (a) but not in helium (b) blobs.

a significant fraction of the charge separation in hydrogen, but not in helium, in agreement with previous results [7].

The importance of the present results, in particular for fusion, is further amplified by similarities between blobs and ELM filaments, which suggest that the same mechanism is governing their dynamics [28]. Recent measurements reveal parallel currents associated with filaments during ELMs [4], which result in large net currents to divertor plates [29]. These currents perturb magnetic probes and affect machine operation, and may cause changes in the magnetic topology [30]. The origin and detailed spatial structure of these currents (monopolar [3,31] versus dipolar [32]) are a matter of debate. It is interesting to discuss the importance of the parallel current caused by the polarization of the filament and its asymmetric structure. An estimate of the net current (assuming a circular filament of radius r) is $I \approx (\alpha - 1)J^{+} \times r^2\pi$, where the exact value of α (in our case $\alpha \approx 2.7$) depends upon the ratio eV_{fl}/T_e. In the SOL of tokamaks, typical filament parameters are $c_s \sim$ 30–60 km/s, $n_e \sim 1$–3×10^{19} m^{-3} and $r \sim 1$–3 cm. Net currents in the range $\approx$ 50–500 A should be expected, which are of the order of measured filament currents [33].

In summary, we presented the first experimental 2D measurements of profiles of parallel current associated with plasma blobs in a simple magnetized toroidal device. 2D dipolar structures of both floating potential and current density were measured. While the floating potential is almost a perfectly symmetric dipole, this is not the case for the current density, which exhibits a stronger lobe on the side dominated by electron currents. This is due to the nonlinear dependence of the total current upon the floating potential. The relevance of the parallel current density asymmetry to ELM filaments was also discussed. Using internal measurements, we showed the existence of two regimes for blob propagation, in which parallel currents to the sheath, respectively, do (in hydrogen) or do not (in helium) efficiently damp the ∇B and curvature induced polarization of the blob.

We thank B. P. Duval, B. Labit, and P. Ricci for insightful discussions. This work is partly supported by the *Fonds National Suisse de la Recherche Scientifique* and by the European Communities, under the contract of Association between EURATOM/ENEA, within the framework the European Fusion Development Agreement.

[1] J. Park *et al.*, Ann. Geophys. **28**, 697 (2010).
[2] M. Spolaore *et al.*, Phys. Rev. Lett. **102**, 165001 (2009).
[3] A. Kirk *et al.*, Phys. Rev. Lett. **96**, 185001 (2006).
[4] N. Vianello *et al.*, Phys. Rev. Lett. **106**, 125002 (2011).
[5] C. Silva *et al.*, Plasma Phys. Controlled Fusion **51**, 105001 (2009).
[6] H. Takahashi, E. Fredrickson, and M. Shaffer, Phys. Rev. Lett. **100**, 205001 (2008).
[7] C. Theiler *et al.*, Phys. Rev. Lett. **103**, 065001 (2009).
[8] N. Katz *et al.*, Phys. Rev. Lett. **101**, 015003 (2008).
[9] S. Krasheninnikov, Phys. Lett. A **283**, 368 (2001); O. E. Garcia *et al.*, Phys. Plasmas **12**, 090701 (2005); J. Myra and D. D'Ippolito, Phys. Plasmas **12**, 092511 (2005).
[10] A. Fasoli *et al.*, Plasma Phys. Controlled Fusion **52**, 124020 (2010).
[11] I. Furno *et al.*, Phys. Rev. Lett. **100**, 055004 (2008).
[12] M. Podestà *et al.*, Phys. Rev. Lett. **101**, 045001 (2008).
[13] M. Podestà *et al.*, Plasma Phys. Controlled Fusion **47**, 1989 (2005).
[14] P. Ricci and B. N. Rogers, Phys. Rev. Lett. **104**, 145001 (2010).
[15] P. Ricci *et al.*, Phys. Plasmas **18**, 032109 (2011).
[16] S. H. Müller *et al.*, Phys. Plasmas **14**, 110704 (2007).
[17] C. Theiler *et al.*, Phys. Plasmas **15**, 042303 (2008).
[18] S. H. Müller *et al.*, Phys. Plasmas **13**, 100701 (2006).
[19] R. H. Cohen and D. D. Ryutov, Phys. Plasmas **2**, 2011 (1995).
[20] M. F. M. De Bock *et al.*, in *Proceedings 37th EPS Conference on Plasma Physics, Dublin* (IOP Publishing, Bristol, 2010).
[21] J. V. Allen, Am. J. Phys. **74**, 809 (2006).
[22] H. Johnsen, H. Pecseli, and J. Trulsen, Phys. Fluids **30**, 2239 (1987).
[23] I. Furno *et al.*, Phys. Plasmas **15**, 055903 (2008).
[24] P. Stangeby, *The Plasma Boundary of Magnetic Fusion Devices* (Inst. of Phys. Pub., Berkshire, 2000), ISBN 0-7503-0559-2.
[25] S. I. Krasheninnikov *et al.*, J. Plasma Phys. **74**, 679 (2008).
[26] D. A. D'Ippolito *et al.*, "Convective Transport by Intermittent Blob-Filaments: Comparison of Theory and Experiment," Phys. Plasmas (to be published).
[27] D. A. D'Ippolito *et al.*, Phys. Plasmas **9**, 222 (2002).
[28] D. L. Rudakov *et al.*, Nucl. Fusion **45**, 1589 (2005); M. Endler *et al.*, Plasma Phys. Controlled Fusion **47**, 219 (2005); W. Fundamenski *et al.*, Plasma Phys. Controlled Fusion **49**, R43 (2007).
[29] J. Lingertat *et al.*, J. Nucl. Mater. **241**, 402 (1997); R. Pitts *et al.*, Nucl. Fusion **43**, 1145 (2003); T. Eich *et al.*, J. Nucl. Mater. **337**, 669 (2005).
[30] A. Wingen *et al.*, Phys. Rev. Lett. **104**, 175001 (2010).
[31] J. R. Myra, Phys. Plasmas **14**, 102314 (2007).
[32] V. Rozhansky and A. Kirk, Plasma Phys. Controlled Fusion **50**, 025008 (2008).
[33] P. Migliucci *et al.*, Phys. Plasmas **17**, 072507 (2010); A. Kirk *et al.*, Plasma Phys. Controlled Fusion **48**, B433 (2006).